

Gas pockets and hydraulic jumps in pressurised pipelines

(Void fraction measurements with optical fibre probes)

ABSTRACT

In practice, it proves to be difficult to completely degas pipelines or to ensure that free gas is not entrained in the pipeline during operation. A recent inventory among water boards in the Netherlands showed that half of the wastewater pressure lines suffered from an increased pressure loss for no obvious reason. Reduction of the system's nominal capacity can be the result of many causes; increased wall roughness, scaling or the occurrence of gas pockets. Gas pockets are formed either by degassing of dissolved gas or by air entrainment at the pumps' inlet or at air valves. In practice, stagnant air pockets and subsequent hydraulic jumps will occur frequently since the required critical velocity is higher than the actual flow velocity. This paper describes some results of void fraction measurements performed at a facility designed for investigation of air pockets and hydraulic jumps. Experiments have been conducted to investigate the influence of pipe inclination, flow velocity on the distribution of air downstream of the hydraulic jump. The objective is to obtain a better understanding of the possible flow modes in gas/water mixtures and characteristics of hydraulic jumps in pressurized pipes. Based on there results, eventually, a model can be defined with which it is possible to simulate air/gas pockets in pipelines.

Keywords: multiphase flow, optical fiber probe, hydraulic jump, void fraction

INTRODUCTION

A previous study (Lubbers et al., 2004) showed that a fairly large flow velocity is necessary to avoid gas pocket from accumulating at high points in pressurized pipelines. In practice, stagnant gas pockets and subsequent hydraulic jumps formation occurs frequently. In wastewater pressure mains however, the occurrence of hydraulic jumps is not deliberate since they reduce the capacity of the system. It was also shown that hydraulic jumps act as transportation mechanism, as it breaks up the large air pocket into small bubbles having a different drag to buoyancy ratio. By choosing the optimum inclination angle and flow velocity in the design phase, accumulated air can be broken down and removed in an efficient way during periods of larger flow rates. Hydraulic jumps in channels have been studied thoroughly by numerous researchers. Their application in channels as a means of flow control is well understood. Hydraulic jumps in pressurized pipes show a variety of different modes of air transport. The distribution of air in the hydraulic jump is determined by measuring the void fraction at several locations with optical fiber probes using a high sampling frequency. The void fractions are measured for a range of Froude numbers, inclination angles and distances from the foot of the jump. The objective is to obtain a better understanding of the possible flow modes in gas/water mixtures and characteristics of hydraulic jumps in pressurized pipes.

METHODS AND MATERIAL

The experiments have been conducted in a two-phase test circuit. The facility comprises a perspex test section that consists of a horizontal approach section, a negative sloping section, followed by a

horizontal discharge part. The angle of the inclined part may be varied in the range of 5° and 40° , of which in this stage OFP measurements have been conducted at 5° and 30° .

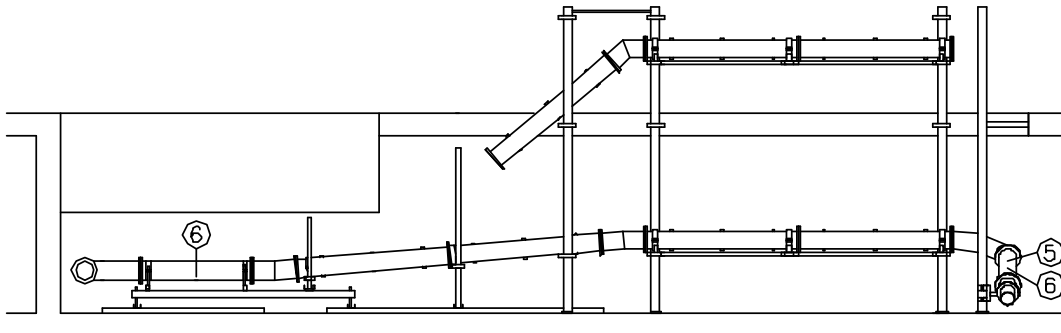


Figure 1. Side view of test section

The inside diameter of the Perspex pipes is 220 mm. The water flow is produced by a pump and is controlled by a control PC that communicates with an EM flow meter and a control valve. The airflow is injected upstream of the test section by a combined flowmeter / flow control valve that receives air from a 6 bar supply system. An optical fibre probe detecting air/water boundaries based on the difference of refractive indices of air and water determines the local void fraction. Two optical fibre probe arrangements are applied at the inclined section opposite to each other, they are mounted on a traverse mechanism to control the location of the tip of the optical fibre probe perpendicular to the axis of the pipe. Its location is read from a scale. Both probes can traverse beyond the centre line allowing for an overlap. The combination of water- and airflow was selected to produce a hydraulic jump upstream of the location of the optical fibre probe. For the 5° angle, measurement series are taken at 40 and 47 l/s and for 30° at 30 l/s and 40 l/s.

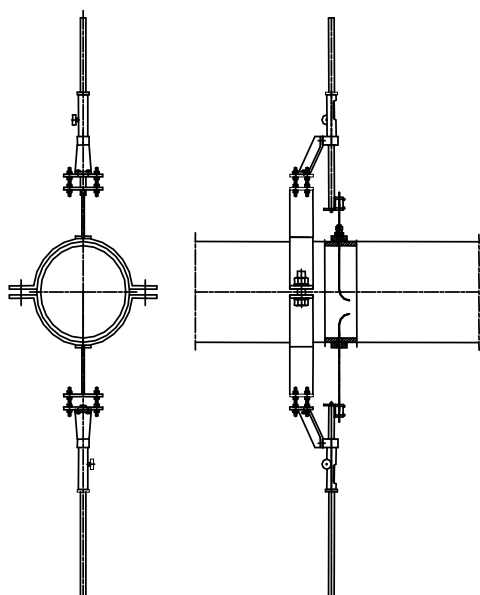


Figure 2. Optical fibre probe arrangement.

Table 1. List of tests

5°		Qw = 40 l/s		
Qa (l/min)	h	x	U	Fr
1.8	0.104	127	2.26	2.24
1.9	0.104	127	2.26	2.24
2.0	0.096	81	2.52	2.60
2.25	0.096	60	2.52	2.60

5°		Qw = 47 l/s		
Qa (l/min)	h	x	U	Fr
6	0.109	100	2.51	2.43
8	0.107	75	2.57	2.51
9	0.107	73	2.57	2.51
10	0.102	45	2.72	2.71

30°		Qw = 30 l/s		
Qa (l/min)	h	x	U	Fr
1.5	0.060	261	3.56	4.64
2.5	0.060	238	3.56	4.64
5.0	0.056	214	3.93	5.30
9.0	0.056	193	3.93	5.30
15	0.058	172	3.74	4.96
25	0.056	141	3.93	5.30

30°		Qw = 40 l/s		
Qa (l/min)	h	x	U	Fr
2	0.118	371	1.93	1.80
3	0.109	353	2.14	2.07
10	0.095	332	2.55	2.64
15	0.090	313	2.72	2.89
25	0.077	291	3.37	3.88

The origin of the reference frame (x, z) is taken at the bottom of the pipe wall, perpendicular to the location of the foot of the hydraulic jump, where the incoming water depth is h . As the water flow rate is kept constant and the flow rate of air is varied, the values of h , U and therefore Froude number vary per series. An overview of the different measurements is given in Table 1.

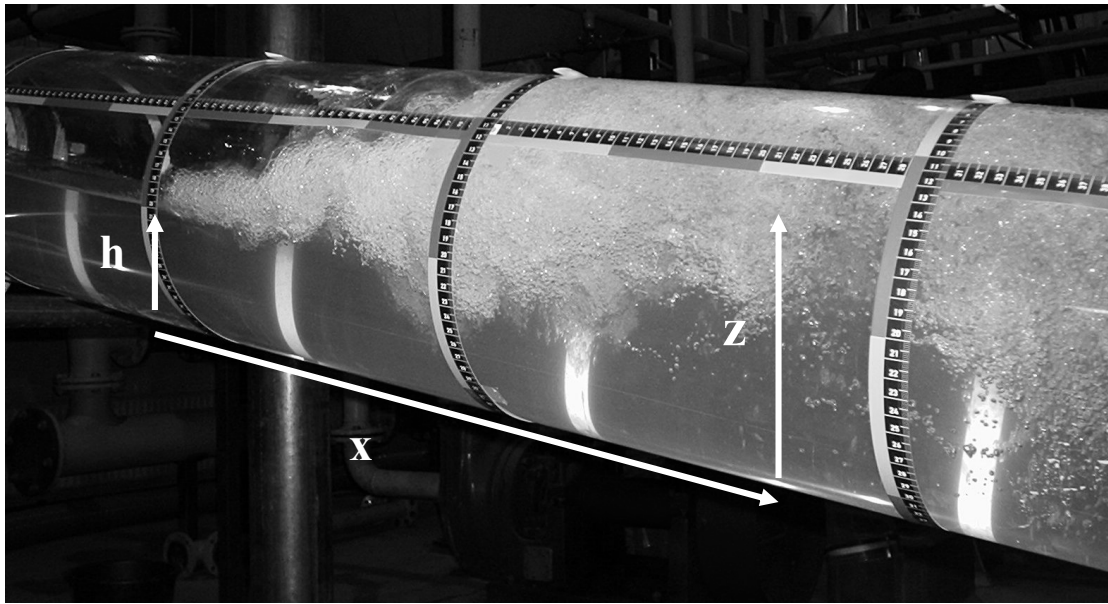


Figure 3. Picture of a hydraulic jump in a closed pipe.

RESULTS AND DISCUSSION

Applied theory

The results are compared with the findings of Murzyn et al. (2004) where possible. The equations to describe the void fraction C is postulated by Chanson (1996) and reads:

$$u \frac{\partial C}{\partial x} + C \frac{\partial u}{\partial x} = \frac{\partial}{\partial z} \left(D \frac{\partial C}{\partial z} \right) \quad (1)$$

u represents the velocity at the foot of the hydraulic jump and D a diffusion coefficient. For the bottom region on a given vertical plane x , the void fraction profile should satisfy the form:

$$C(x, z) = C_{\max} \exp\left(-\frac{1}{4} \frac{U}{D} \frac{(z - z_{c\max})^2}{x}\right), \quad (2)$$

C_{\max} is the maximum void fraction at location $(x, z_{c\max})$. For the upper region of an open channel hydraulic jump a solution given by Brattberg et al. (1998) for the edge of water jets discharging into air is suggested that follows the form:

$$C(x, z) = \frac{1}{2} \left[1 + \operatorname{erf}\left(\frac{z - z_{c50}}{2\sqrt{Dx/U}}\right) \right], \quad (3)$$

which is also a solution to an appropriate diffusion equation. The location where C is $\frac{1}{2}$ is z_{c50} , and C reaches 1 as z goes to infinity. The upper region of the hydraulic jump in a pressurized pipe is bounded by the pipe wall instead of air. Therefore C will never reach unity. However, in the pipe, intermittently, large volumes of air (plugs) flow counter currently to the high point, causing interfacial aeration at the free surface. To what this extent this form is applicable is still questionable.

Void fraction profiles

The parameters of Eqs. (2) and (3) are obtained by fitting their log functions with the Levenberg-Marquart method. The value of C_{\max} is limited to 1, which also implies that in this case the fit does not agree well with Eq.(2). Figure 4 shows the void fraction profile plotted against z at location $x = 0.81$ m ($x/h = 8.4$) for 5° angle and 40 l/s. The transition between the two regions is clearly visible. The maximum void fraction in the hydraulic jump does not reach 1 as does in an open channel. Eqs. (2) and (3) are fitted and plotted on a logarithmic and linear scale respectively. The approximations agree fairly well with the measurement data. The location of the intersection z^* of the two approximations is around 0.15 m.

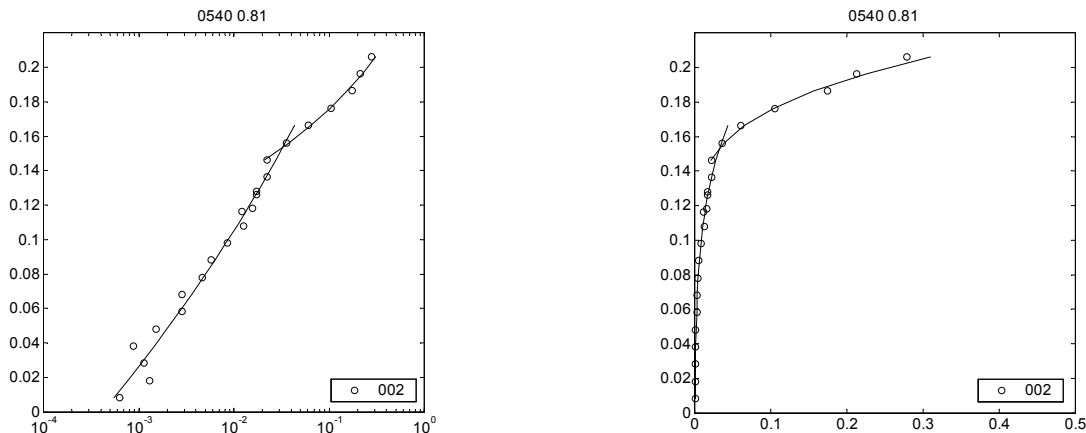


Figure 4. Approximation of the measurements according to Eq. (2) and Eq. (3), logarithmic (left) and linear (right) scale.

In Figure 5 all void fractions mentioned in Table 1 for the 5° angle and 40 l/s are plotted normalized according to Eqs. (2) and (3). The Froude number varies between 2.2 and 2.6, while x/D varies between 2.7 and 5.8. Figure 5 shows that the measured data is in fairly good agreement with the profiles of their respective regions. Void fraction at the top of the lower regions and the bottom of the top regions break away from the trends as the transition between the two regions is approached.

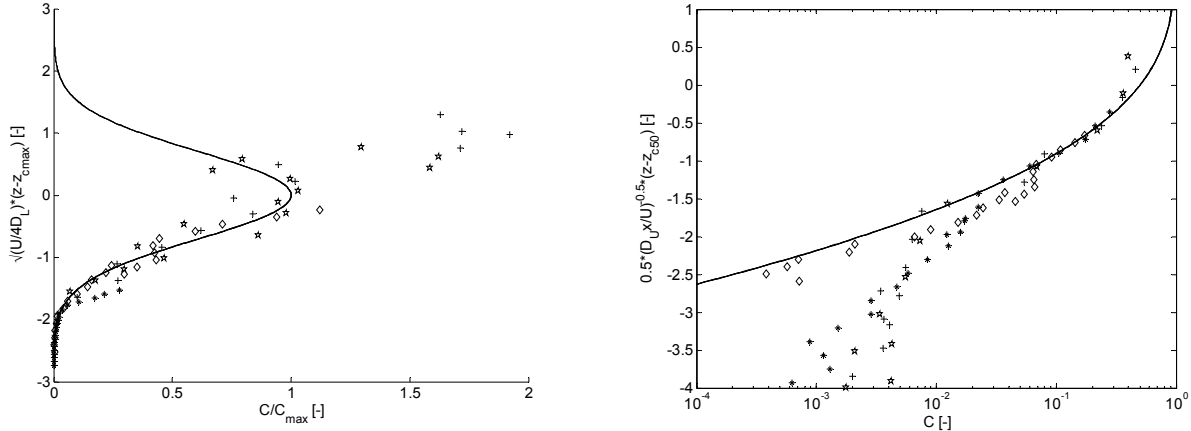


Figure 5. Void fractions plotted against elevations normalized according to Eq. (2) and (3) for top and bottom respectively which are shown as solid lines.

In Figure 8 the fitted parameters of Eq. (2) are plotted against their relative distance x/h from the foot of the hydraulic jump. For C_{max} (top) the results of Murzyn show a decrease in value with increasing distance for constant Froude number. Since x/D cannot be changed without changing Fr , it is not clear from the measurements whether this trend is present. The middle figure shows the values of z_{cmax} .

The bottom shows the values of the diffusion coefficient D . Figure 9 shows the fitted parameters of Eq. (3). Opposite to Murzyn's findings no increase in z_{c50} with distance is present (top). A reason of the z_{c50} being constant may be the fact that the pipe does not allow the hydraulic jump to expand in vertical direction. The bottom figure shows scattered values of the diffusion coefficient D .

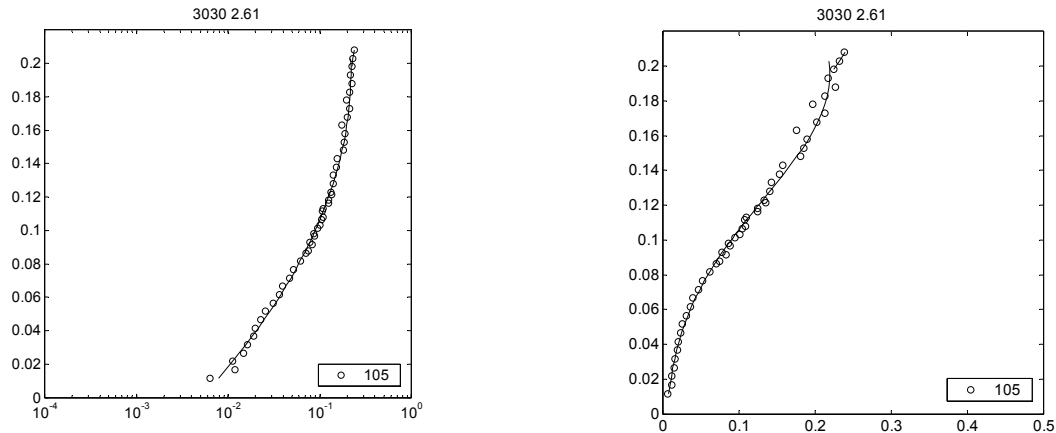


Figure 6. Experimental data of void fraction and approximation on logarithmic scale (left) and logarithmic scale (right).

The void fractions measured at an inclination angle of 30° show a different profile. Figure 6 shows the void fraction for 30 l/s at location $x = 2.61 \text{ m}$ ($x/D = 11.9$) plotted together with the approximations of Eq. (2) and (3). Both visual observations and measurements for the 30° angle show that the air is better mixed over the vertical profile than for 5° . Figure 6 shows that the void fraction profile is almost fully approximated by the lower region equation.

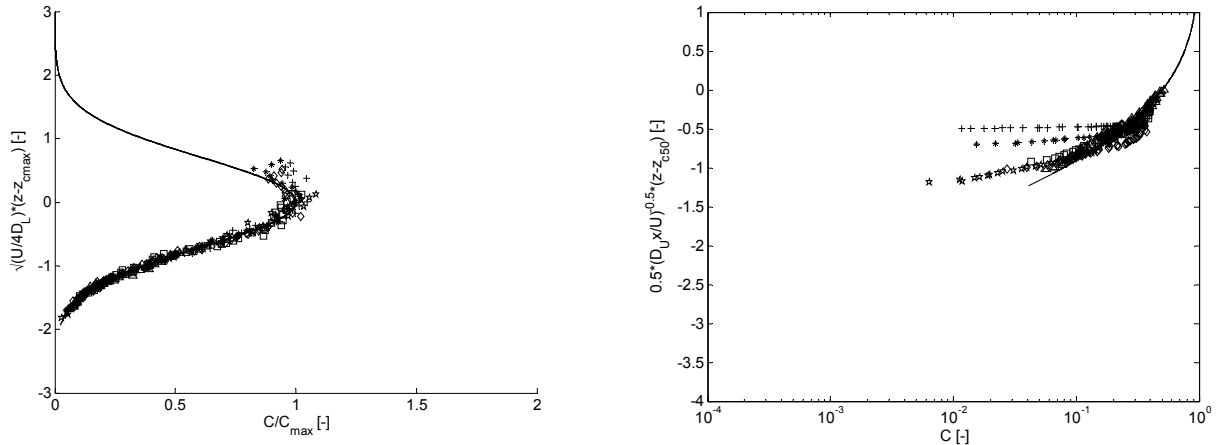


Figure 7. Void fractions plotted against elevations normalized according to Eq. (2) and (3) for top and bottom respectively which are shown as solid lines.

For the hydraulic jump in a pipe with inclination angle of 30° , a sharp edge between upper and lower regions is seen. Figure 7 shows that Eq. (2) for the bottom region almost covers the whole profile, while Eq. (3) of the upper region only covers a small part of the upper part of the profile.

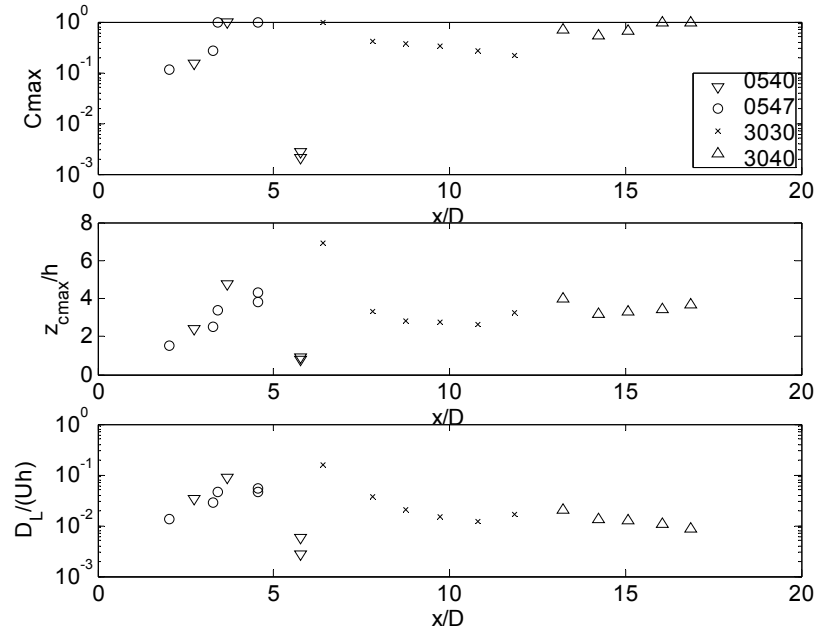


Figure 8. Parameters of the lower region obtained by fitting Eq. (2).

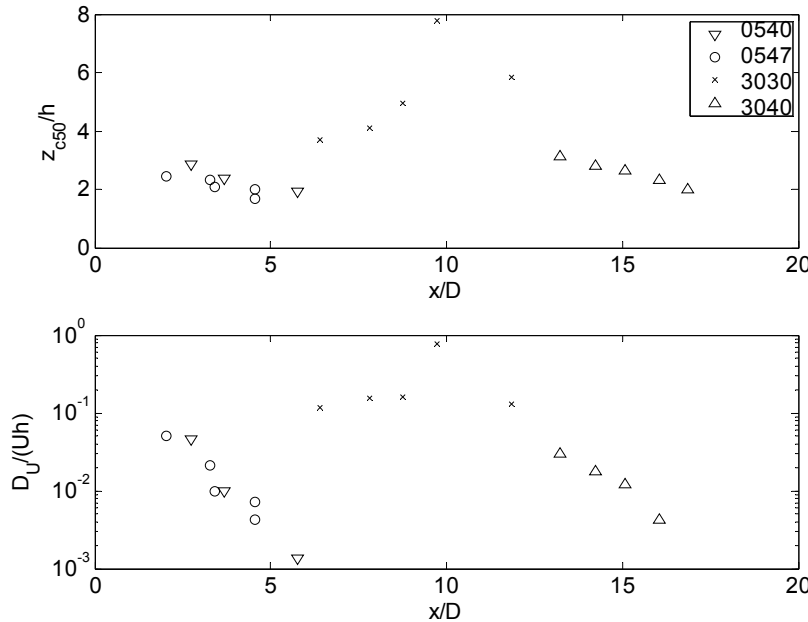


Figure 9. Parameters of the upper region obtained by fitting Eq. (3).

Velocity profile shape (factor)

Assuming that the void fraction profile value is constant at a certain plane x , a fictitious air transport is calculated by multiplying the void fraction as a function of z by the width of the pipe at location z and the average velocity.

$$Q_{\text{air fict}} = \int_{z=0}^D f(z) \cdot w(z) \cdot U_{\text{mean}} dz \quad (4)$$

The resulting air discharges are much greater than the supplied airflow rate. It is observed that intermittently pockets of airflow counter currently back to the high point. Due to buoyancy, air bubbles move against the mean flow direction along the top of the pipe. This results in (temporary) negative velocities at the upper region. This phenomenon does not occur at open channel flow.

A shape factor of the velocity profile is defined that must be present to explain the discrepancy between the supplied airflow rate and the fictive air transport. U_{mean} is replaced by

$$U = \begin{cases} u_c & z < z_{\text{inverse}} \\ u_{cc} & z > z_{\text{inverse}} \end{cases} \quad (5)$$

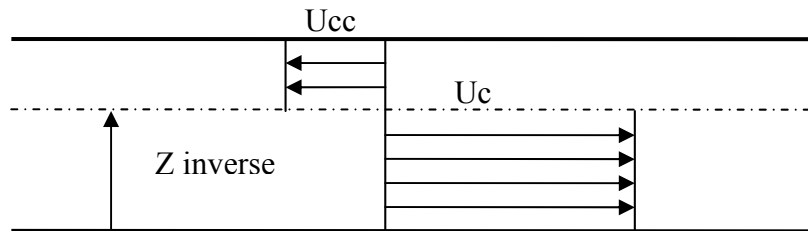


Figure 10 shows the possible combinations of the ratio of u_c and u_{cc} for different locations of z . Figure 11 shows the amount of air transport that would occur as a function of the location of velocity profile inverse. Remarkable is the amount of recirculation that occurs.

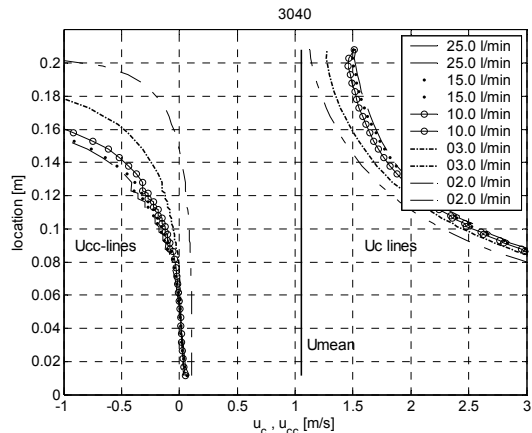


Figure 10. Possible ratios of u_c and u_{cc} as a function of the location z .

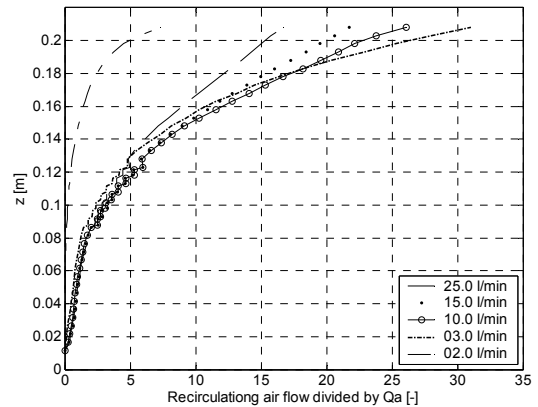


Figure 11. Local air flow rate carried with the flow compared to supplied air flow rate.

CONCLUSIONS AND DISCUSSION

For 5° inclination angle, a similar transition of void fraction regions as in the case of open channel is observed. At 30° the transition could not clearly be identified. The inclination angle has influence on the distribution of air but the absence of a clear transition of the regions is caused by the fact that the measured profile is far from the foot of the hydraulic jump and no aeration of from upper region takes place. The agreement of the void fraction profiles with Eq. (2) however is good. Further research will focus on the assessment of the location $z_{inverse}$ in order to obtain better understanding of the efficiency of the hydraulic jump's ability to transport air. The values of h are assessed by reading a ruler that has been attached to the circumference of the pipe. The water level corresponds to a circumference value that is converted to water depth, the readings have the best accuracy for water levels at the centre line of the pipe and worsen towards the bottom or top, because of refraction of light at the curved pipe.

ACKNOWLEDGEMENT

The study is carried out by the University of Delft and Delft Hydraulics in collaboration with the majority of the water boards in the Netherlands and two consultancy companies.

REFERENCES

- Brattberg T., Toombes L., Chanson H., (1998) Developping air-water shear layers of two-dimensional water jets discharging into air. *Proc. FEDSM'98: ASME Fluids Engineering Division Summer Meeting, Washington DC*.
- Chanson H. (1996). Air bubble entrainment in free surface turbulent flows. Academic Press.
- Lubbers C.L., Clemens F. H.L.R. (2005). Air pockets in sewerage pressure mains. *Water Science and Technology*, **52** (3), pp 37-44
- Murzyn F., Mouaze D., Chaplin J.R. (2004). Optical fibre probe measurements of bubbly flow in hydraulic jumps. *Int. J. Multiphase Flow*, **31** (2004), pp. 141 – 154.